Journal of Engineering Science and Technology Review 17 (2) (2024) 52 - 57

Research Article

JOURNAL OF
Engineering Science and Technology Review

www.jestr.org

Evolution Characteristics of Multi-physical Fields in Dissolved Surrounding Rockmass of Tunnel Considering Fluid-solid Coupling

Shifan Liang[1], Chunhai Li[2,*], Jiaqi Guo[1] and Erbo Wang[1]

[1]*School of Civil Engineering, Henan Polytechnic University, Jiaozuo 454003, China*
[2]*Institute of Defense Engineering, Academy of Military Science, Beijing, 100850, China*

Received 12 September 2023; Accepted 23 February 2024

Abstract

To explore the evolution characteristics of multi-physical fields in dissolved surrounding rockmass during karst tunnel construction, a tunnel engineering calculation model with multiple karst caves were constructed by using the partical flow code (PFC). The parallel bond model was situated among the molecules forming a block cementing material similar to rock. Under the combined action of excavation disturbance and karst water pressure, the evolution characteristics of multi-physical fields in karst cave surrounding rock during karst cave formation were analyzed, including the displacement field, stress field, and seepage field. Results show that the presence of a karst cave stratum increases the displacement around the tunnel and significantly reduces the integrity of the surrounding rockmass. The final displacement value of the tunnel vault is higher than that of its left and right sides. After unloading, the stress field of the surrounding rockmass increases significantly due to dissolution, leading to a significant stress concentration around the karst cave. The cracks initiate and expand rapidly, with the stress concentration occurring at the arch bottom being the most significant. At the same time, a stable seepage field is formed in the surrounding rockmass. The conclusions obtained in this study provide the scientific and practical values for reducing and controlling the occurrence of water inrush disasters during karst tunnel construction.

Keywords: Dissolved surrounding rockmass, Multi-physical fields, Discrete element method, Evolution characteristics

1. Introduction

With the continuous advancement of the “Belt and Road” initiative and the successive implementation of major projects such as the Sichuan-Tibet Railway, the new land and sea passage in the west, the national water network, and the hydropower development in the lower reaches of the Yarlung Zangbo River, China has begun to gradually move towards becoming a strong transportation country. Especially the transportation infrastructure in the western region has entered a new period of rapid development [1]. However, the western region is mostly a gathering area of carbonate rock strata. Under the combined action of multiple factors, karst landforms are widely distributed and exist in various types. The complex karst geological environment has posed significant challenges to the safe construction of the tunnel, especially the water gushing and mud inrush resulting from karst engineering geological problems. Adverse geological disasters such as surface subsidence and karst development are highly concealed and complex. The consequences of disasters significantly impact the advancement of normal tunnel construction, leading to project shutdowns and even route alterations.

Due to the complex geological environment in karst areas tunnel survey and design are challenging, the requirements for environmental and water resources protection are high, leading to significant construction safety concerns and high operational costs. Once the tunnel has structural safety problems or diseases during operation, it will pose significant challenges to traffic flow and disease maintenance [2-4]. The karst tunnel refers to the rockmass of a karst cave with a specific pore structure that develops over time due to natural factors such as karst groundwater and climate. The formation of the karst cave disrupts the integrity of the surrounding rockmass, thereby impacting the mechanical properties of the surrounding rockmass. The water inrush disaster mainly occurs in the early stages of karst development. The external dynamic disturbance alters the dissolution effect of the surrounding rockmass. The existence of the karst cave is the primary cause of geological disasters, such as karst water inrush and collapse, during the construction of the tunnel [5, 6].

Under the combined action of factors such as tunnel excavation and construction disturbance, the initial stress equilibrium state in the surrounding rockmass of the tunnel is broken, the stress redistribution phenomenon occurs in the surrounding rockmass, and the stability of the surrounding rockmass is obviously reduced, resulting in water inrush and water inrush during tunnel construction, increase of surrounding rockmass pressure, dissolution development of surrounding rockmass, dissolution cavity, increase of internal force of lining structure, etc., which brings certain challenges to the construction and operation of tunnel engineering, and even engineering diseases. In order to prevent all kinds of karst geological disasters in tunnel construction in karst areas, it is of great significance to study the evolution characteristics of the surrounding rockmass of karst tunnels during construction for tunnel safety in karst areas and it is also the scientific and technological requirements for tunnel construction and safe operation in China's transportation infrastructure.

*E-mail address: hubeilichunhai@sina.com
ISSN: 1791-2377
doi:10.25103/jestr.172.07

2. State of the Art

In recent years, many scholars have carried out a large number of effective numerical simulation studies on the evolution characteristics of displacement field, stress field, and seepage field of surrounding rockmass of karst tunnels [7-9]. For the displacement field characteristics of surrounding rockmass, Gao et al. [10] studied the evolution characteristics of the displacement field of surrounding rockmass with different cave sizes during tunnel excavation. Ma et al. [11] studied the effects of various cave locations, sizes, and distances on the displacement evolution characteristics of karst tunnels surrounding rockmass. Sheinin et al. [12] studied the settlement law of surrounding rockmass of karst tunnel through numerical simulation and analyzed the causes of surrounding rockmass deformation. Golian et al. [13] proposed a method to evaluate the discharge time after tunnel water inrush and analyzed the variation characteristics of displacement following tunnel water inrush. Yau et al. [14] proposed a risk assessment method for karst tunnels, which predicted the displacement deformation of surrounding rockmass and the stability of supporting structure. Li et al. [15] investigated the impact of hidden karst caves on the displacement characteristics of karst caves. Compared with karst cave tunnels, the deformation of the surrounding rockmass of the cave vault during tunnel excavation is more pronounced.

For the characteristics of surrounding rockmass stress field, Zhang et al. [16] studied the variation in stress of karst tunnels with different height-span ratios. It is concluded that with the increase in height-span ratio, the principal stress of surrounding rockmass increases, and the change in vault principal stress occurs in the surrounding rockmass. Huang et al. [17] conducted a comparative analysis of the effect of various cave widths and filling degrees on the stress evolution characteristics of the supporting structure. Chen et al. [18] studied the effect of concealed karst caves in different locations on the stress field and seepage field of surrounding rockmass, and obtained the variation law of stress in karst caves. Mahmoudi and Rajabi [19] researched the impact of the clear distance between the karst cave and the tunnel on the stress evolution characteristics of the supporting structure. They pointed out that the bearing capacity of supporting structure decreases as the clear distance between the tunnels increases.

For the characteristics of surrounding rockmass seepage field, Gangrade et al. [20] proposed a method based on geostatistical modeling to quantitatively assess the risk of karst voids in tunnel projects in karst geological environments. Tarifard et al. [21] studied and analyzed the influence of rock creep behavior and groundwater on the long-term stability of karst tunnel surrounding rockmass. Herrera et al. [22] established a groundwater depth monitoring system for karst tunnels, which served as a foundation for predicting tunnel water inrush disasters. Liu et al. [23] studied the water inrush characteristics of karst tunnels under overlying confined pressure, indicating that the rock mass between the surrounding rockmass and the tunnel is prone to overall sliding instability. Ashjari et al. [24] studied the permeability of the surrounding rockmass of karst tunnels and showed that the permeability of the tunnel spandrel is the most obvious.The above studies simulated the effect of karst caves on the evolution characteristics of the tunnel's surrounding rock mass under different conditions. However, the simulated karst cave are all single karst cave, while there are multiple karst caves of varying sizes and scales in the dissolved surrounding rockmass of the tunnel.

Based on the current research situation, the partical flow code (PFC) was utilized to study the impact of multiple karst caves on the evolution characteristics of the surrounding rock mass. The research focused on the evolution of the displacement field, stress field, and seepage field of dissolved surrounding rockmass during karst cave formation [25, 26]. The results have significant implications for uncovering the stress and permeability characteristics of surrounding rockmass and for the formation of karst tunnels and caves.

The rest of this study is arranged as follows. In Section 3, the principle of fluid-solid coupling calculation and the establishment of numerical model of dissolved surrounding rockmass are expounded. In Section 4, the results of corroded surrounding rockmass are analyzed and described. Finally, the conclusion is summarized in Section 5.

3. Methodology

3.1 Fluid-solid coupling principle in PFC

To understand the fluid-solid coupling between fluid and particles, the contact model of particles is considered to parallel bond model. The parallel bond model is situated among the molecules, which will form a block cementing material similar to rock. In discrete element computations, the fluid typically occupies the gaps between solid particles, and fluid q flows to the fluid domain P through interconnected fluid channels, simulating the real situation of rock seepage. Schematic diagram of liquid flow in the fluid domain is shown in Fig. 1.

3.2 Computational model for dissolved surrounding rockmass based on PFC

The PFC software is used to construct the numerical calculation model. The calculation process mainly involves the following steps: (1) Generating the particle numerical computation model; (2) Fully compacting the particles; (3) Adjusting the stress inside the particles; (4) Deleting the suspended particles inside the model; (5) Applying bonding strength to the particles; (6) Adjusting the stress state of the particles inside the model. The numerical model of the tunnel in this study has dimensions of 5 m × 5 m. To investigate the effect of multi-cave strata on the evolution characteristics of the tunnel surrounding rockmass, the tunnel is simplified. The tunnel contour is set as a circular structure with a diameter of 0.3 m. The coordinate origin depends on the center of the model.

The displacement constraints are applied to the left and right boundaries of the model. The bottom boundary is an impermeable boundary, while the upper boundary is a permeable boundary. The boundary conditions and monitoring point settings of the model are shown in Fig. 2.

There are eight monitoring points arranged in the vault (A), spandrels (B, H), hances (C, G), arch footings (D, F) and arch bottom (E) of karst tunnel. The macroscopic and microscopic parameters of the dissolved surrounding rockmass are obtained through the parameter calibration method [27]. The density of discrete element particles is 2700 kg/m^3, the contact modulus between particles is 59.2 GPa, and the friction coefficient between particles is 0.7. The rockmass has an elastic modulus of 65 GPa and a Poisson's ratio of 0.27.

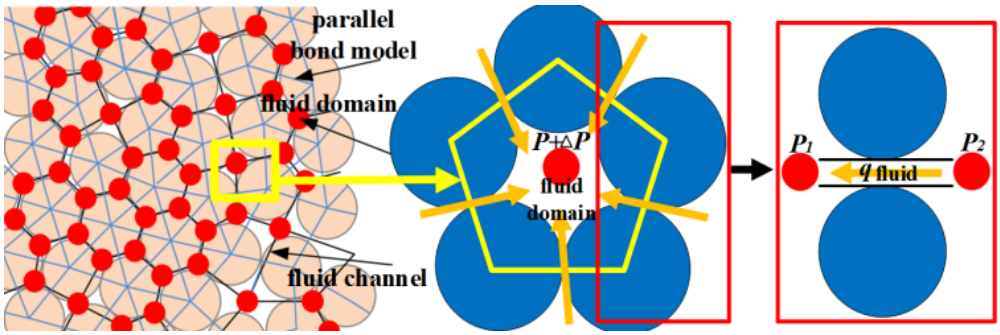

Fig. 1. Schematic diagram of liquid flow in fluid domain.

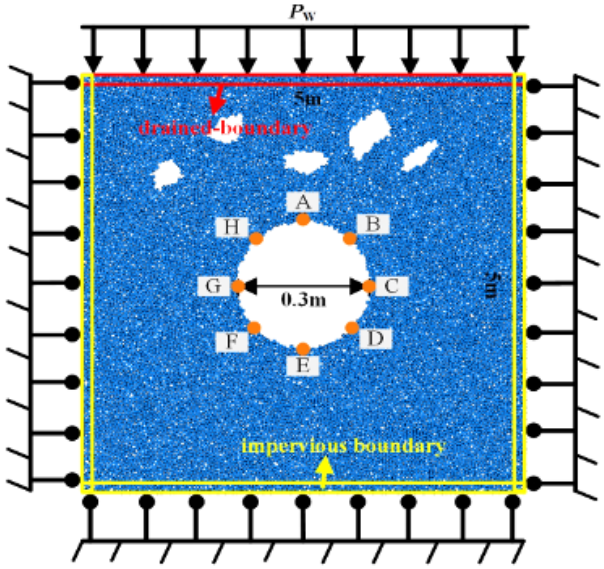

Fig. 2. Boundary conditions and monitoring point settings of model.

4. Results Analysis and Discussion

4.1 Evolution characteristics of displacement field

Fig. 3 shows the evolution characteristics of displacement field. There are multiple karst caves of various sizes formed in the dissolved surrounding rockmass. When the numerical simulation computation step increases from 500 steps to 1500 steps, the displacement in the dissolved surrounding rockmass gradually goes up, especially around the karst cave. However, the increase in displacement is not significant. As the time step of numerical computation gradually raisings to 2000 steps, the integrity of the surrounding rock mass is compromised due to the presence of a karst cave in the dissolved surrounding rockmass. Consequently, the displacement field of the surrounding rockmass undergoes significant changes. When the numerical computation time step is 4500 steps, the displacement value of the tunnel vault is 1.32 cm.

In comparison with the calculation time step of 3500 steps, the vault's displacement value raisings by 18.4 %. Due to the existence of the karst cave, the stability of the surrounding rockmass is significantly reduced. During tunnel excavation, the tunnel vault should be supported at all times to insure the safety of the tunnel construction.

Fig. 4 shows the displacement evolution characteristics of monitoring points. It can be seen from Fig. 4 that when the numerical time step is 1500 steps, the displacement of the karst tunnel vault is 0.32 cm, which is 28.2 % higher than when the time step is 500 steps. As the calculation time step is further increased to 3500 steps and 4500 steps, the vertical displacement of the surrounding rockmass gradually increases. The growth rate of vertical displacement becomes more significant, pointing that the internal stress equilibrium state of the dissolved surrounding rockmass is gradually disrupted due to the interaction of excavation disturbance and karst water pressure. Consequently, the internal stress of the surrounding rockmass is redistributed. With the gradual raising of the time step, the displacement change at each monitoring point also increases gradually. The displacement change value at the tunnel vault is notably higher than at other positions.

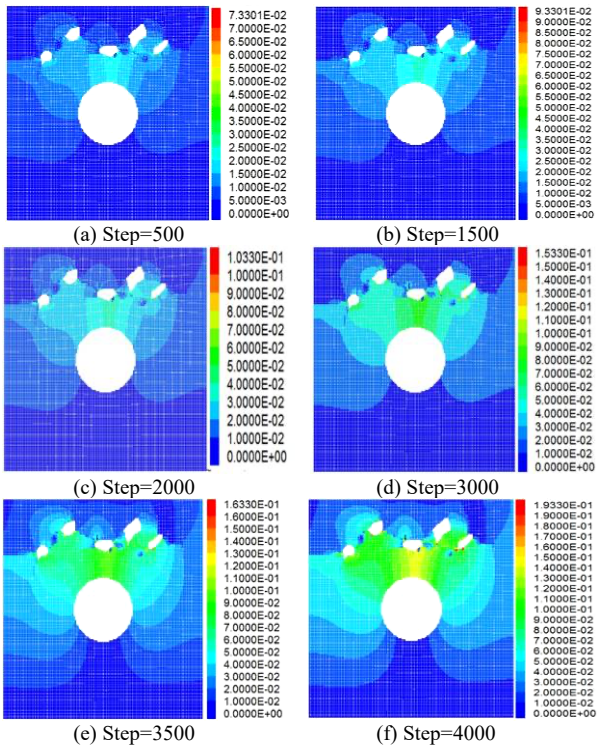

Fig. 3. Evolution characteristics of displacement field.

As the time step increases, the displacement of the vault becomes more and more significant. The displacement values at each monitoring point from largest to smallest are as follows: vault (A) > spandrel (B) > hance (C) > arch footing (D) > arch bottom (E). The displacement value of the tunnel vault is 1.32 cm, which is 19 % higher than that of the right spandrel. The impact of karst water pressure and the continuous disturbance caused by tunnel excavation significantly affect the surrounding rockmass at the vault, making it more susceptible to collapse and instability.

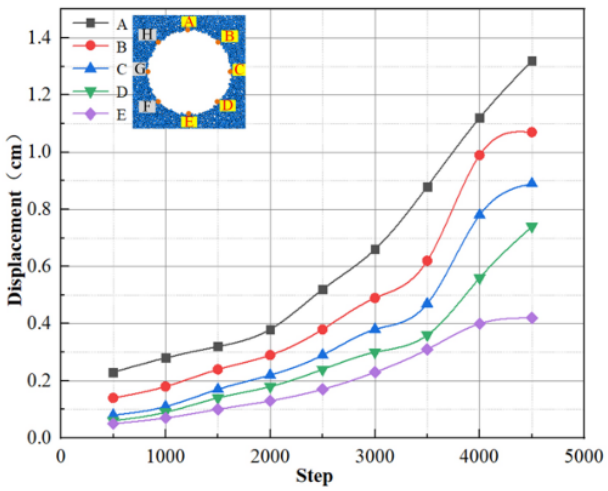

Fig. 4. Displacement evolution characteristics of monitoring points.

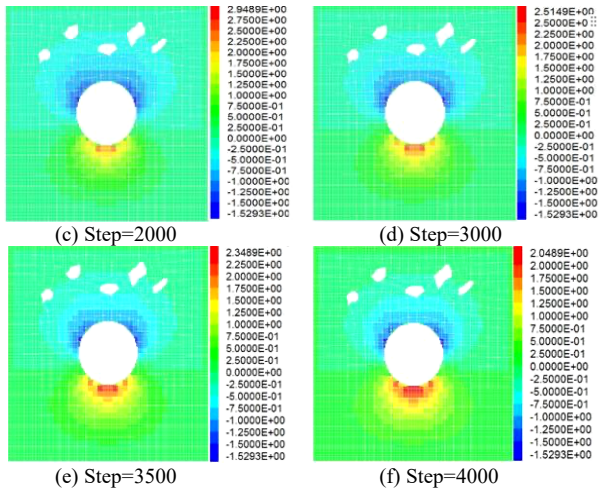

Fig. 5. Evolution characteristics of stress field.

4.2 Evolution characteristics of stress field

Fig. 5 shows the evolution characteristics of stress field. It can be seen from Fig. 5 that at the numerical calculation time step is 500 steps, due to the effect of excavation unloading, the stress of the surrounding rockmass, and the initial stress state around the karst cave is disrupted, leading to significant stress concentration around the karst cave. As the numerical calculation time step raisings to 2000 steps, the combined effect of external loads and karst water pressure will lead to the release of stress in the surrounding rockmass. Consequently, the stability of the surrounding rockmass will be significantly reduced, causing rapid initiation and expansion of cracks around the karst cave.

When the numerical calculation time step is 500 steps, the stress value of the arch footing is 0.68 MPa. In comparison with the calculation time step of 4500 steps, the stress in the vault increases by 10.3 %. Due to the presence of karst caves, the integrity of the surrounding rockmass is compromised. After excavation, the internal stress field of the surrounding rock mass significantly increases compared to the stress condition before excavation.

It can be seen from Fig. 6 that as the numerical calculation time step increases, the stress value at each monitoring point gradually rises. The stress state of the arch footing and arch bottom is mainly compressive. Compared to the arch footing, the arch footing has a higher compressive stress value. The stress state of the vault, spandrel, and hance is mainly tensile. Compared with the vault and spandrel, the tensile stress value of the hance is larger. At the beginning of tunnel excavation, the initial stress balance of the surrounding rock mass is disrupted due to excavation disturbance, leading to stress redistribution around the tunnel. The final stress value at the bottom of the arch is 2.23 MPa. In comparison with the arch footing, the stress value increases by 57 %, indicating that the stress redistribution phenomenon is more significant at the arch bottom.

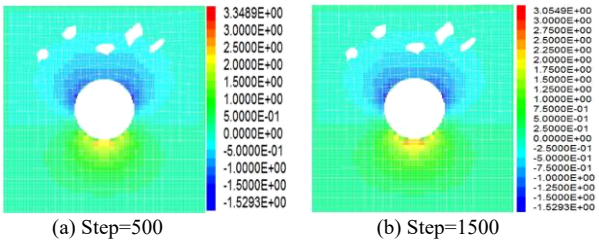

As the number of time steps in the numerical calculation increases to 2000 steps, the stress in the surrounding rockmass accumulates continuously due to the persistent action of karst water pressure and excavation unloading. At the same time, the presence of dissolution pores compromises the integrity of surrounding rockmass. The stress at the bottom of the tunnel arch increased from 1.04 MPa during the initial stage of excavation to 2.23 MPa, representing a 53% increase in stress value. Therefore, the stability of the surrounding rockmass is significantly reduced by unloading during tunnel excavation, leading to rapid initiation and expansion of cracks around the dissolved pore structure. Among these, the change in the stress at the bottom of the arch is more obvious, and stress redistribution is likely to occur during the construction process.

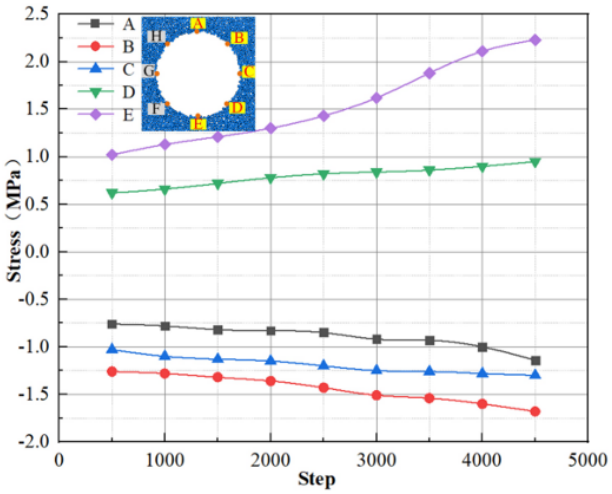

Fig. 6. Stress evolution characteristics of monitoring points.

4.3 Evolution characteristics of seepage field

Fig. 7 shows the evolution characteristics of seepage field. It can be seen from Fig. 7 that as the numerical calculation time step increases, the seepage area in the dissolved surrounding rockmass increases significantly due to the continuous action of excavation unloading. Before the tunnel excavation, the dissolved surrounding rockmass has formed a stable seepage field due to the influx of karst water pressure. During the excavation and unloading of the karst tunnel, the seepage water pressure increases, especially affecting the rocks around the tunnel opening. The karst water gradually penetrates into the vault, arch bottom, and spandrel of the tunnel through the cracks. Due to the

presence of karst caves in the dissolved surrounding rockmass, the stability of the surrounding rockmass is significantly reduced, while its permeability is greatly enhanced. This leads to a notable difference between the seepage water pressure of the fissure water and the water pressure before excavation.

When the numerical calculation time step is set to 500 steps, karst water pressure and excavation disturbance can lead to the formation of cracks in the rock mass around the tunnel vault, due to the presence of karst caves. However, these cracks do not propagate all the way to the surface, and there is no formation of a macroscopic fissure water channel within the rock layer. With the successive increase in the time step to 2000 steps, the seepage damage to the rock mass gradually worsens due to the effects of excavation unloading and seepage water pressure. This leads to the initiation and propagation of cracks in the surrounding rockmass, causing the flow velocity within the surrounding rockmass to gradually raising. As the numerical calculation time step raisings to 4500 steps, the stability of the rock around the tunnel further decreases. With the interaction of excavation disturbance, internal cracks expand quickly and form a macroscopic fissure water channel. Due to the pressure of karst water, it flows rapidly into the tunnel, causing further destruction to the entire surrounding rockmass.

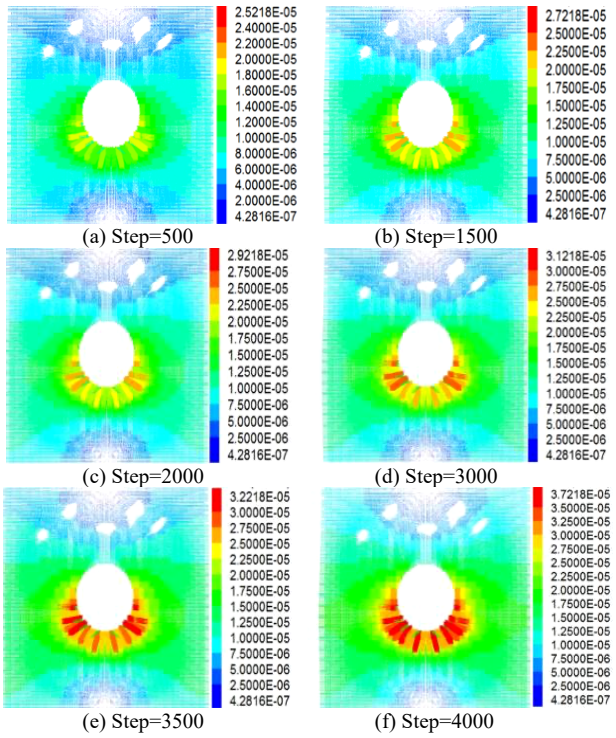

Fig. 7. Evolution characteristics of seepage field.

Fig. 8 shows the seepage evolution characteristics of monitoring points. It can be seen from Fig. 8 that as the numerical calculation time step increases, the seepage water pressure of each monitoring well continuously rises. The seepage water pressure at the arch footing reaches its maximum value, and the water pressure at the bottom of the arch and the hance is essentially equal. The vault's water pressure from seepage is the lowest. When the calculation time step is 1500 steps, the seepage water pressure at the bottom of the arch is 2.15 MPa. When the calculation time step is 3000 steps, the seepage water pressure at the bottom of the arch is 3.12 MPa, which is 45.11 % higher than that at 1500 steps. When the calculation time step is 4500 steps, the seepage water pressure at the bottom of the arch is 3.69 MPa, which is 18.26 % higher than that at 3000 steps.

With the increase in the numerical calculation time step, the seepage water pressure at the bottom of the tunnel surrounding rockmass rises significantly. The above phenomena show that with the interaction of excavation disturbance and karst water pressure, the stability of karst tunnel arch bottom is compromised. Consequently, the size of cracks formed in the surrounding rockmass is larger, and their connectivity is stronger.

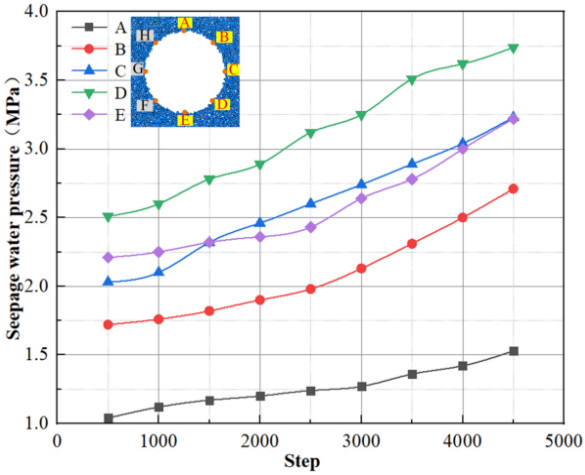

Fig. 8. Seepage evolution characteristics of monitoring points.

5. Conclusions

In this study, the characteristics of the displacement field, stress field, and seepage field of dissolved surrounding rockmass under the interaction of excavation disturbance and karst water pressure are investigated using the PFC software. The main conclusions are obtained as following:

(1) The existence of karst cave stratum increases the displacement around the tunnel karst cave and significantly reduces the integrity of the surrounding rockmass. As the numerical calculation time step increases, the growth rate of the surrounding rock mass displacement also increases. The final displacement values of each monitoring point from largest to smallest are as follows: vault, spandrel, hance, arch footing, arch bottom. The vault's final displacement value is higher than that of its left and right sides.

(2) The stress state of the vault, spandrel, and hance is mainly tensile, while the stress state of the arch footing and arch bottom is primarily compressive. After the tunnel excavation and unloading, the stress field of the surrounding rockmass increases significantly. There is a significant stress concentration phenomenon around the karst cave, where cracks initiate and propagate rapidly. Among these, the stress concentration at the arch bottom is the most significant.

(3) As the numerical calculation time step increases, the seepage failure of the tunnel intensifies, and the internal flow velocity gradually rises. The seepage area and water pressure of the corroded surrounding rockmass have significantly increased. The water pressure reaches its maximum in the arch footing, while it is the smallest in the vault. At the same time, a stable seepage field forms within the surrounding rockmass.

The study on the evolutionary characteristics of dissolved surrounding rockmass is of great significance in revealing the evolution process of seepage and penetration in

dissolved surrounding rockmass. In the next step, the mechanical failure mechanism of rock mass with varying degrees of dissolution and the development and evolution characteristics of internal cracks should be investigated. Additionally, the evolution of permeability and mechanical properties of dissolved surrounding rockmass under different degrees of dissolution will be further studied.

Acknowledgements

This study was financially supported by the National Natural Science Foundation of China (52178388) and the China Postdoctoral Science Foundation Fund (2018M631114).

References

[1] L. P. Li, Z. Y. Zhu, Z. Q. Zhou, S. S. Shi, Y. X. Chen, and W. F. Tu, "Calculation methods of rock thickness for preventing water inrush in tunnels and their applicability evaluation," *Chin. J. Rock Mech. Eng.*, vol. 41, no. 1, pp. 41-50, Jul. 2020.

[2] Z. H. Xu, L. Peng, H. L. Xing, D. D. Pan, and X. Huang, "Hydro-mechanical coupling response behaviors in tunnel subjected to a water-filled karst cave," *Rock Mech. Rock Eng.*, vol. 54, no. 8, pp. 3737-3756, May. 2021.

[3] Y. C. Zheng, S. Y. He, Y. Yu, J. Y. Zheng, Y. Zhu, and T. Liu, "Characteristics, challenges and countermeasures of giant karst cave: A case study of Yujingshan tunnel in high-speed railway," *Tunn. Undergr. Sp. Tech.*, vol. 114, pp. 103988, Aug. 2021.

[4] K. Zhang, Z. L. Zhou, and S. G. Chen, "Stability Assessment of Ground Surface along Tunnels in Karst Terrain Using Improved Fuzzy Comprehensive Evaluation," *Adv. Civ. Eng.*, vol. 05, pp. 1-13, Apr. 2021.

[5] M. Ćuk, I. Jemcov, and A. Mladenović, "Hydrochemical impact of the hydraulic tunnel on groundwater in the complex aquifer system in Pirot, Serbia," *Carbonate. Evaporite.*, vol. 35, no. 31, pp. 1-17, Apr. 2020.

[6] X. Huang, S. Li, Z. Xu, M. Guo, and Y. Chen, "Assessment of a concealed karst cave's influence on karst tunnel stability: a case study of the Huaguoshan tunnel," *Sustainability,* vol. 10, no. 7, pp. 2123, Sep. 2018.

[7] S. R. Wang, M. C. He, and Z. W. Liu. "Analysis of the process of water burst catastrophe and it's prevention counter-measures in a karst tunnel," *J. Uni. Sci. Technol. Beijing*, vol. 28, no. 7, pp. 613-618, Jul. 2006.

[8] Z. C. Li, Z. Z. Yang, S. R. Wang, L. W. Ren, and J. Fang. "The effects of coal floor brittleness on the risk of water inrushes from underlying aquifers: a numerical study," *Sustainability*, vol. 16, no. 4, pp. 1489, Feb. 2024.

[9] S. R. Wang and H. Wang. "Water inrush characteristics with roadway excavation approaching to fault," *Telkomnika*, vol. 10, no. 3, pp. 505-513, Jul. 2012.

[10] J. Q. Gao, Y. Qian, J. X. Chen, and F. Chen "The minimum safe thickness and catastrophe process for water inrush of a karst tunnel face with multi fractures," *Processes*, vol. 7 no. 10, pp. 686, Nov. 2019.

[11] J. J. Ma, J. W. Guan, J. F. Duan, L. C. Huang, and Y. Liang, "Stability analysis on tunnels with karst caves using the distinct lattice spring model," *Undergr. Space*, vol. 06, no. 4, pp. 469-481, Aug. 2021.

[12] V. I. Sheinin, A. V. Anikeev, A. D. Kochev, and O. A. Korol, "Analysis of causes and geomechanical schematization of catastrophic karst subsidence development," *Soil Mech. Found. Eng.*, vol. 60, no. 4, pp. 348-355, Nov. 2023.

[13] M. Golian, M. Abolghasemi, and A. Hosseini, "Restoring groundwater levels after tunneling: a numerical simulation approach to tunnel sealing decision-making," *Hydrogeol. J.*, vol. 29, no. 4, pp. 1611-1628, Apr. 2021.

[14] K. Yau, C. Paraskevopoulou, and S. Konstantis. "Spatial variability of karst and effect on tunnel lining and water inflow. A probabilistic approach," *Tunn. Undergr. Sp. Tech.*, vol. 97, pp. 103248, Mar. 2020.

[15] S. C. Li, J. Wu, Z. H. Xu, L. Zhou, and B. Zhang, "A possible prediction method to determine the top concealed karst cave based on displacement monitoring during tunnel construction," *B. Eng. Geol. Environ.*, vol. 78, no. 23, pp. 341-355, Aug. 2019.

[16] L. W. Zhang, H. Fu, and J. Wu. "Effects of Karst Cave Shape on the Stability and Minimum Safety Thickness of Tunnel Surrounding rock," *Int. J. Geomech.*, vol. 21, no. 9, pp. 234-241, Oct. 2021.

[17] F. Huang, L. H. Zhao, T. H. Ling, and X. L. Yang, "Rock mass collapse mechanism of concealed karst cave beneath deep tunnel," *Int. J. Rock Mech. Min.*, vol. 91, no. 4, pp. 133-138, Feb. 2017.

[18] Y. C. Chen, C. Y. Wang, and M. Guo, "Effect of concealed karst cave on surrounding rock stability and its treatment technology," *J. Shandong Univ., Eng. Sci.*, vol. 50, no. 5, pp. 33-43, Sep. 2020.

[19] M. Mahmoudi and M. Rajabi. "A numerical simulation using FLAC^{3D} to analyze the impact of concealed karstic caves on the behavior of adjacent tunnels," *Nat. Hazards*, vol. 117, no. 1, pp. 555-577, Feb. 2023.

[20] R. M. Gangrade, J. G. Grasmick, and M. A. Mooney, "Probabilistic assessment of void risk and grouting volume for tunneling Applications," *Rock Mech. Rock Eng.*, vol. 55, no. 6, pp. 2771-2786, Sep. 2022.

[21] A. Tarifard, P. Görög, and Á. Török, "Long-term assessment of creep and water effects on tunnel lining loads in weak rocks using displacement-based direct back analysis: an example from northwest of Iran," *Geomech. Geophys. Geo.*, vol. 31, no. 8, pp. 1-15, Feb. 2022.

[22] R. G. Herrera, M. C. Cepeda, and S. Pinto. "A homogeneous approach in modeling a coastal karst aquifer," *Earth Sci. Inform.*, vol. 15, no. 03, pp. 1825-1840, Jul. 2022.

[23] H. Liu, Z. Lin, B. Zhang, C. Wang, J. Liu, and H. Liang, "Stability analysis of karst tunnels based on a strain hardening-softening model and seepage characteristics," *Sustainability*, vol. 14, no. 15, pp. 89-95, May. 2022.

[24] J. Ashjari, F. Soltani, and M. Rezai, "Prediction of groundwater seepage caused by unclogging of fractures and grout curtain dimensions changes via numerical double-porosity model in the Karun IV River Basin," *Environ. Earth Sci.*, vol. 78, no. 85, pp. 324-347, Aug. 2019.

[25] J. H. Yang, S. R. Wang, H. Q. Zhang and C. Cao. "Particle-scale analysis of key technologies of the cut-and-cover tunnel on the slope," *J. Eng. Sci. Technol. Rev.*, vol. 7, no. 4, pp. 46-52, Oct. 2014.

[26] S. R. Wang, J. A. Wang, S. H. Liu, S. C. Wu, and J. W. Xie. "Particle flow analysis on mechanized top-coal caving in steep thick seam," *J. Uni. Sci. Technol. Beijing*, vol. 28, no. 9, pp. 802-812, Sept. 2006.

[27] P. Geng, Z. K. Lu, and T. Ding, "Research on the dynamic process simulation of rock grouting based on particle flow," *J. Railw. Eng. Soc.*, vol. 34, no. 3, pp. 34-40, Sep. 2017.